Effect of non-Hermiticity on adiabatic elimination in coupled waveguides

Rahman Sharaf,[1] Mojgan Dehghani,[2] and Hamidreza Ramezani[2,*]
[1]*Faculty of Electrical and Computer Engineering, Tarbiat Modares University, Tehran 14115, Iran*
[2]*Department of Physics and Astronomy, University of Texas Rio Grande Valley, Brownsville, Texas 78520, USA*

(Received 4 June 2017; published 31 January 2018)

We investigate the influence of non-Hermiticity on the adiabatic elimination in coupled waveguides. We show that although the total norm of the system is not conserved in parity-time symmetric phase, the dark state intensity remains constant. However, in broken phase the eliminated waveguide loses its darkness, i.e., its field amplitude starts increasing. In both exact and broken phases, the effective Hamiltonian derived from the adiabatic elimination condition describes the dynamics of all states except the dark state. Specifically, it cannot predict the amplification in the intensity of the dark state. Our results can strengthen the control of the dynamics in cavities with active elements and improve the design of controllable absorbers.

DOI: 10.1103/PhysRevA.97.013854

I. INTRODUCTION

The demand for designing miniaturized and on-chip optical devices with new functionalities has increased in the past few years. Many linear and nonlinear structures such as nanosized fabricated waveguides [1], spherical and disk microresonators [2], photonic crystals [3], and metamaterials [4] have been proposed. In a related matter of finding new structures, non-Hermitian systems have recently become the center of attention in photonics [5–8], electronics [9], and acoustics [10–13] due to their fascinating features and applications [14–19]. Among the non-Hermitian systems, parity and time reversal (PT) symmetric systems are especially important because they show a phase transition from the exact phase with a real spectrum to the broken phase with a complex spectrum [20]. The transition point is known as the exceptional point or the PT-symmetry breaking point. At the exceptional point, two or more eigenvectors of the system in a pairwise manner coalesce, and their associated eigenvalues become degenerate. In each phase, many interesting features have been discovered and demonstrated experimentally. Among them are unidirectional invisibility [21,22], parity anomaly [23], loss-induced lasing [24], protected bound states [25,26], and non-Hermiticity induced flatbands [27,28].

Despite all these achievements, designing nanosized PT structures is very difficult. From a practical standpoint, PT structures are composed of some gain and loss mechanisms that are judiciously distributed in the structure. Usually in such systems, there are some modes that are coupled with each other through coupling constants generated by the overlap integral of the field. In the absence of the couplings, the modes are degenerate and the degeneracy breaks by introducing the coupling. The level spacing between coupled modes is proportional to the coupling, which dictates the bandwidth of the system. The introduction of gain and loss reduces the level spacing until the system reaches the spontaneous symmetry breaking point where the level spacing becomes zero. Thus, when the coupling between the modes is stronger, the bandwidth of the system becomes wider, and consequently the exact phase of the PT system becomes larger. On the other hand, in nanoscale and densely packed subwavelength structures such as coupled single-mode waveguides, where each mode exists in one waveguide, the fabricated waveguides are very close to each other [29]. The PT version of the densely packed subwavelength waveguides involves gain and loss waveguides. While the loss is usually generated by metal coating [30], the gain is created using optical or electrical pumping. However, in subwavelength structures, the diffraction limit (in the case of optical pumping) or tunneling of electrons and diffusion current (in the case of electrical pumping) poses a major barrier in advancing the field of non-Hermitian photonics in a subwavelength regime and fabricating PT-symmetric densely packed structures. Similar issues are encountered when we deal with densely coupled laser cavities with different gain thresholds. In both cases, pumping a gain site will affect the near-neighboring waveguides or cavities. Thus it is highly desired to find a way to keep coupled gain and loss waveguides away from each other and pump the gain site without affecting the near coupled loss site.

Here we propose to bypass the above problem using the concept of adiabatic elimination (AE). In AE we set the parameters of a system such that the intensity (or population probability) in at least one of the elements (or states) of the structure, which we refer to here as the dark state, remains almost constant [29]. For example, let us consider the three coupled waveguides in Fig. 1. If we want the middle waveguide to be the dark state, then we set couplings and propagation constants such that the intensity in the middle waveguide remains constant during the propagation of the electric field in the waveguide. The dark state will participate in the dynamics by transferring the field from the left outer waveguide to the right one and vice versa. However, its intensity does not change during this process. In this work, we will show that as long as we are in the exact phase this picture is correct and the

*hamidreza.ramezani@utrgv.edu

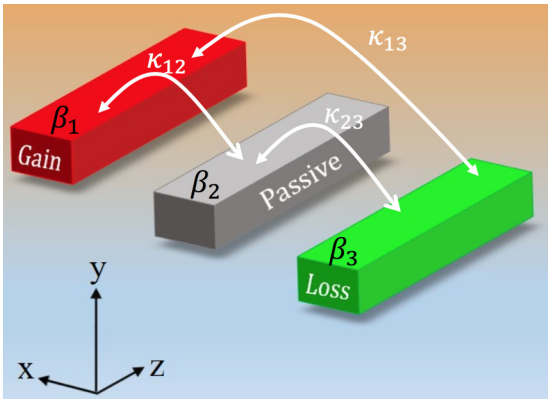

FIG. 1. Schematic of the trimer coupled waveguides. The green waveguide is a loss waveguide, the blue one is gain, while the middle waveguide is considered to have no gain or loss. In AE, one wants to cause the electric field intensity in the middle waveguide to be zero.

intensity of the dark state remains constant, while in the broken phase its intensity amplifies exponentially. Toward that end, we will find the condition for AE in three PT-symmetric coupled waveguides: one with gain, a centric waveguide with no gain or loss, and a loss waveguide. We derive the condition in which the system supports AE and can be effectively described by a 2×2 effective Hamiltonian. Such a Hamiltonian leads us to identify the exact phase and the broken phase. Furthermore, we analyze the beam dynamics in such a PT system and then show that while the intensity of the passive waveguide in the exact phase does not change significantly, in the broken phase the field intensity increases exponentially in all the waveguides. Although we consider coupled waveguides, our approach can be generalized to other systems such as coupled electronic oscillators, acoustic Helmholtz resonators, and absorbers. It should be mentioned that PT-symmetric adiabatic elimination does not lead to a more compact systems. It offers an effective way to generate PT-symmetric dimers from trimers where one can pump the gain site without affecting the loss site.

II. ADIABATIC ELIMINATION CONDITION IN PT-SYMMETRIC COUPLED WAVEGUIDES

Let us consider three coupled waveguides as shown in Fig. 1. The left waveguide with propagation constant $\beta_1 = \beta_1' - i\gamma$ is the gain waveguide, and the right waveguide with propagation constant $\beta_3 = \beta_3' + i\gamma$ is the loss waveguide. Parameter γ identifies the value of the gain and loss. The middle waveguide is a passive waveguide with $\beta_2 = \beta_2'$ and zero gain or loss. The couplings between the waveguides are given by κ_{12}, κ_{23}, and κ_{13} as indicated in Fig. 1. The PT symmetry condition forces the following relations:

$$\beta_1' = \beta_3' \equiv \beta', \quad \kappa_{12} = \kappa_{23} \equiv \kappa. \tag{1}$$

With a good approximation, we can write the couple mode equations describing the propagation of the electric field $\vec{E} = (E_1 \quad E_2 \quad E_3)^T$ along the dimensionless propagation distance z, which is normalized in units of coupling length κ:

$$i\frac{d}{dz}\vec{E} = \begin{pmatrix} \beta_1 & 1 & \kappa_{13} \\ 1 & \beta_2 & 1 \\ \kappa_{13}^* & 1 & \beta_3 \end{pmatrix}\vec{E}. \tag{2}$$

Above we scaled all the parameters and normalized them to the coupling strength κ. Writing the above equations in terms of electric-field amplitudes $E_j = A_j \exp(i\beta_j z)$, we get

$$i\frac{d}{dz}\vec{\psi} = H\vec{\psi}, \quad \vec{\psi} = (A_1 \quad A_2 \quad A_3)^T, \tag{3}$$

where $A_{j=1,2,3}$ represents the electric-field amplitude in gain ($j = 1$), passive ($j = 2$), and loss ($j = 3$) waveguides, respectively. In the Schrödinger-like equation (3), the Hamiltonian H is given by

$$H = -\begin{pmatrix} 0 & e^{-i\Delta\beta_{12}z} & \kappa_{13}e^{-i\Delta\beta_{13}z} \\ e^{i\Delta\beta_{12}z} & 0 & e^{-i\Delta\beta_{23}z} \\ \kappa_{13}^* e^{i\Delta\beta_{13}z} & e^{i\Delta\beta_{23}z} & 0 \end{pmatrix}, \tag{4}$$

where $\Delta\beta_{ij} = \beta_i - \beta_j$, and $*$ denotes conjugation.

Let us assume that we are searching for a condition (the AE condition) that causes the middle waveguide to become a dark state at any z. Thus, we expect that its amplitude, namely A_2, is not influenced by the field of the gain and loss waveguides and remains constant. Consequently, we can integrate the middle row of Eq. (3), which results in

$$A_2 = \frac{1}{\Delta\beta_{12}}e^{i\Delta\beta_{12}z}A_1 - \frac{1}{\Delta\beta_{23}}e^{-i\Delta\beta_{23}z}A_3. \tag{5}$$

From Eq. (5), we can conclude that the AE condition, which makes A_2 a dark sate, is given by

$$1 \ll \sqrt{(\beta' - \beta_2')^2 + \gamma^2}. \tag{6}$$

We can conclude from Eq. (6) that if the AE condition is satisfied for the Hermitian case [29], namely $\gamma = 0$, it is automatically satisfied for the non-Hermitian case with $\gamma \neq 0$.

By making one waveguide a dark state, AE effectively reduces the number of the differential equations in (3) from three to two. Replacing Eq. (6) in Eq. (3) and using Eq. (1), one can write a Schrödinger-like equation that describes the dynamics in the outer waveguides,

$$i\frac{d}{dz}\tilde{\psi} = -\mathcal{H}_{\text{eff}}\tilde{\psi}, \quad \tilde{\psi} = (A_+, A_-)^T, \tag{7}$$

where $A_{+,-} \equiv A_{1,3}\exp(\pm i\Delta\beta_{13}z/2)$. The elements of the Hamiltonian $\mathcal{H}_{\text{eff}} = \begin{pmatrix} \beta_{\text{eff}+} & \kappa_{\text{eff}} \\ \kappa_{\text{eff}}^* & \beta_{\text{eff}-} \end{pmatrix}$ are

$$\beta_{\text{eff}\pm} = \frac{1}{\beta' - \beta_2' \pm i\gamma} \pm i\gamma, \quad \kappa_{\text{eff}} = \kappa_{13} + \frac{1}{\Delta\beta_{12}}. \tag{8}$$

From Eqs. (8) and (6), we observe that to the first-order approximation, the imaginary parts of the propagation constants are not affected by AE, while the couplings have been changed.

We can use $\mathcal{H}_{\text{eff}}$ to identify the exact phase of the coupled waveguides in the AE regime. Specifically, for $\kappa_{13} = 0$, the eigenvalues of $\mathcal{H}_{\text{eff}}$ are given by

$$\mathcal{E}_{1,2} = \frac{\beta' - \beta_2' \pm \sqrt{\Lambda}}{(\beta' - \beta_2')^2 + \gamma^2}, \tag{9}$$

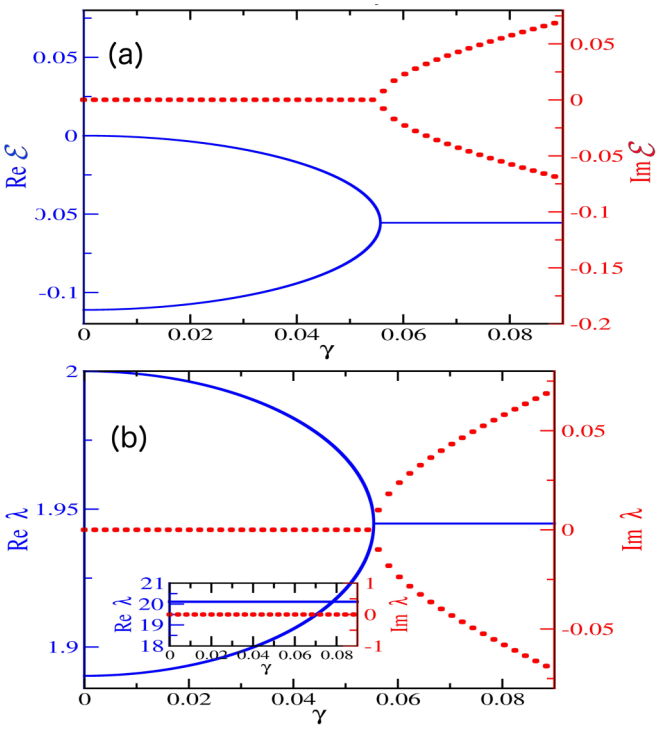

FIG. 2. (a) Real parts (blue curve) and imaginary parts (red dots) of the eigenvalues of $\mathcal{H}_{\rm eff}$ vs γ. (b) Spectrum of Eq. (2) vs γ. A comparison shows that the effective system after the AE approximation accurately describes the exact and broken phase of the system.

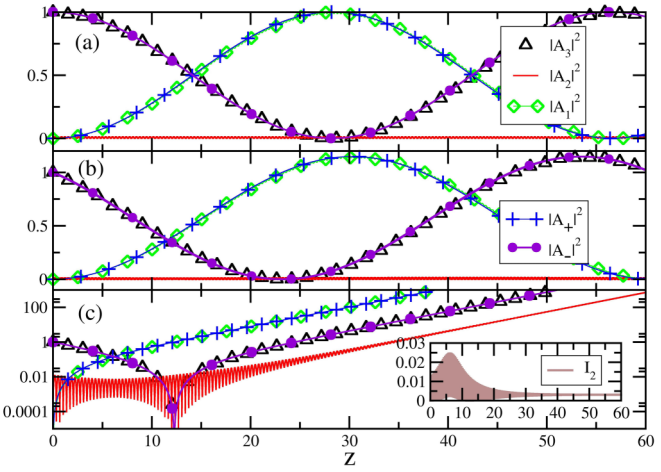

FIG. 3. (a) Beam dynamics in a Hermitian trimer shown in Fig. 1 in the AE regime with $\kappa_{13} = 0$, $\beta_2' = 20$, and $\beta' = 2$. The field from waveguide A_3 transfers into waveguide A_1 while the intensity of the middle waveguide is close to zero. The curves indicated with • and + are the results of integration of effective differential, Eq. (7). (b) Similar to (a) with $\gamma = 0.02$ and in the exact phase. (c) Similar to (a) with $\gamma = 0.14 > \gamma_{\rm PT}$. In this case, AE is not preserved and the field intensity in the middle waveguide increases.

where $\Lambda \equiv (\beta'-\beta_2')^2-\gamma^2[(\beta'-\beta_2')^2+\gamma^2]^2 + 2\gamma^2[(\beta'-\beta_2')^2 + \gamma^2]$. Obviously, our structure is in the exact phase for $\Lambda > 0$. In the upper panel of Fig. 2, we plotted the real and imaginary parts of the eigenvalues of $\mathcal{H}_{\rm eff}$, namely $\mathcal{E}$, versus gain and loss parameter γ for $\beta' = 2$, $\beta_2' = 20$, and $\kappa_{13} = 0$. The lower panel of Fig. 2 depicts the spectrum, λ, of Eq. (2) versus γ. Three modes $\lambda_{1,2,3}$ are shown, where two of them, $\lambda_{1,2}$, are in the main panel. The dark mode λ_3 is demonstrated in the subfigure. A comparison between the upper and lower panels of Fig. 2 shows that Eq. (9) accurately predicts the spontaneous symmetry breaking point at $\gamma \equiv \gamma_{\rm PT} = 0.055$. Thus, from a numerical perspective, one can use the AE approximation to reduce the dimensionality of the system to identify the spontaneous symmetry breaking point. Despite its accuracy in finding the exceptional point, $\mathcal{H}_{\rm eff}$ does not describe the spectrum of the coupled waveguides. We see a shift in the position of the two predicted modes $\lambda_{1,2}$ in the spectrum. In the next section, we show that in the exact phase, this shift is not important and the dynamics is described by the difference between the upper and lower levels, the so called bandwidth. Figure 2 depicts that the bandwidth after the AE approximation is preserved, $|\lambda_1 - \lambda_2| = |\mathcal{E}_1 - \mathcal{E}_2| = \frac{2\sqrt{\Lambda}}{(\beta'-\beta_2')^2+\gamma^2}$. In contrast, in the broken phase the imaginary part of λ describes the actual exponential increase in the intensity of the field. Figure 2 shows that the imaginary branches are the same in both parts (a) and (b). Thus, the imaginary branches of the eigenvalues in Fig. 2(a) describe the exponential decay and growth of the modes of the system when we satisfy Eq. (6). This result is not trivial, as initially we began our calculations with the assumption that the A_2 does not change during the evolution.

III. DYNAMICS

Armed with previous knowledge about the eigenmode properties of the PT-symmetric trimer in the AE regime, we proceed to study beam dynamics. The question is to determine whether Eq. (7) describes the dynamics in both exact and broken phase and how the dynamics is affected by the value of non-Hermiticity under the AE condition.

To answer the above question, we first excite the loss waveguide in Fig. 1 for different values of the gain and loss parameter γ under the condition given in Eq. (6), and we check the electric-field propagation along the z direction. Now, let us consider the Hermitian case in which $\gamma = 0$. In this case [Fig. 3(a)], the approximation that we are using works with a high accuracy, and Eq. (7) shows the same dynamics as the actual system described by the set of differential equations in Eq. (3). The excitation in the right waveguide in Fig. 1 couples to the left waveguide, while the intensity in the middle one (dark state) remains almost zero. In Fig. 3(b), we introduce the gain and loss such that $0 < \gamma < \gamma_{\rm PT}$. We observe that while the overall dynamics is affected by the gain and loss as discussed in Ref. [31], the AE approximation describes the dynamics very well. Similar to the Hermitian case, the intensity in the middle waveguide remains zero. In the exact phase due to the bi-orthogonality of the eigenvectors, the total norm is not conserved. However, the total intensity in the system remains bounded with power oscillation. Finally, in Fig. 3(c), we increase $\gamma > \gamma_{\rm PT}$ such that the system enters into the broken phase. Although two sets of differential equations (3) and (8) predict the same dynamics, the intensity in the passive waveguide increases. Consequently, one can conclude that the intensity of the dark state does not remain constant, and the AE

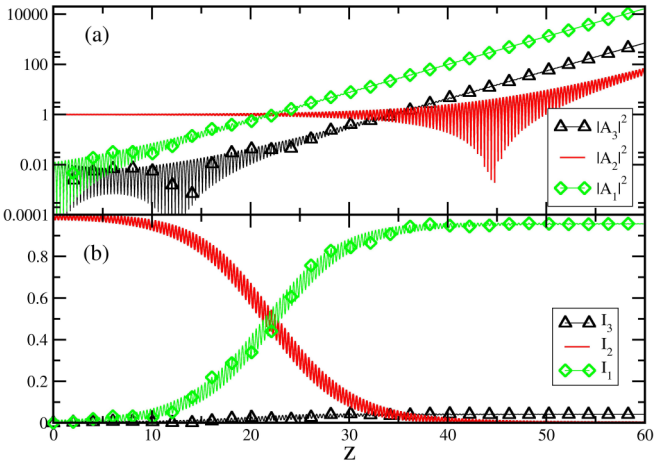

FIG. 4. (a) Beam dynamics in the broken phase when the dark sate (middle waveguide) is excited, with $\kappa_{13} = 0$, $\beta_2' = 20$, and $\beta' = 2$. The intensity in the gain (green curve) and loss waveguide (black curve) increases exponentially. (b) Relative intensities associated with part (a). We observe that the relative intensity in the middle waveguide tends to zero and does not remain constant.

effect does not hold in terms of constant intensity. Specifically, in the exact phase from H_{eff} and H one can calculate the total norm of the system, while in the broken phase the total norm cannot be calculated via H_{eff}.

The exponential growth in all three waveguides depicted in Fig. 3(c) might infer that although the intensity of the middle waveguide does not remain constant, the relative intensity of the middle waveguide, namely $I_i = \frac{|A_i|^2}{|A_1|^2+|A_2|^2+|A_3|^2}$ $(i = 2)$, remains almost zero, and hence if we modify the definition of AE, the AE holds in terms of intensities even in the broken phase. In the inset of Fig. 3 we have plotted the relative intensity for the middle waveguide I_2 when we excite the loss waveguide. We observe that at propagation length $z \approx 6$ coupling units, the relative intensity I_2 has a peak. After the peak, I_2 reaches an almost constant value. We have examined the peak numerically, and we found that its value increases for larger values of γ. However, one might say that by neglecting this peak, the relative intensity remains constant, and thus AE holds in the broken phase if we redefine the AE elimination using the relative intensities. Below, using numerical simulation, we show that this is not correct even if we modify the definition of AE in terms of the relative intensities. Specifically, by applying the AE condition in Eq. (6), we expect that when the middle waveguide is excited, its (relative) intensity does not change while the (relative) intensity of the outer waveguides remains nearly zero and the (relative) intensity of the middle waveguide remains constant. Figure 4(a) depicts the intensity in each waveguide when the middle one is initially excited and the system is in the broken phase with $\gamma = 0.14 > \gamma_{\text{PT}} = 0.055$. We observe that the intensity in all waveguides increases exponentially, meaning that the AE does not hold when we use intensities as a measure for adiabatic elimination. Figure 4(b) depicts the relative intensities $I_{i=1,2,3}$ for the same initial condition and the same parameters as in Fig. 4(a). If AE holds, we expect that the relative intensity of the outer waveguide remains zero. However, we observe that the relative intensity in the gain waveguide increases and saturates to 1, and the relative intensity of the dark sate, namely the middle waveguide, decays and tends to zero. This observation proves that although under the AE condition in Eq. (6) the effective Hamiltonian describes the same dynamics for the left and right waveguide, it cannot describe the total norm in the system.

Physically, in the broken phase as depicted in Fig. 2, the imaginary part of the eigenvalue of one of the modes associated with H becomes positive and the imaginary part of the eigenvalue of the second mode becomes negative while the third eigenvalue associated with the last mode remains real, namely $\lambda_3 \in \text{Re}$. Specifically, the two complex eigenvalues have the following form:

$$\lambda_{1,2} = \lambda_r \pm i\lambda_i \quad \text{with } \lambda_{r,i} \in \text{Re}. \tag{10}$$

The spatial representation of the initial condition can be expanded in term of the corresponding eigenvectors

$$\vec{\psi}(0) = \sum_{j=1}^{3} \alpha_j |\lambda_j\rangle, \tag{11}$$

where $|\lambda_j\rangle = (a_j, b_j, c_j)^T$ with $j = 1,2,3$ are the eigenvectors of the Hamiltonian H in Eq. (3), and a,b,c are in general nonzero parameters. The evolution of the initial excitation in Eq. (11) will be given by

$$\vec{\psi}(z) = \sum_{j=1}^{3} \exp(-i\lambda_j z)\alpha_j |\lambda_j\rangle. \tag{12}$$

The right-hand side of Eq. (12) can be written as

$$e^{(\lambda_i - i\lambda_r)z}\alpha_1|\lambda_1\rangle + e^{(-\lambda_i - i\lambda_r)z}\alpha_2|\lambda_2\rangle + e^{-i\lambda_3 z}\alpha_3|\lambda_3\rangle. \tag{13}$$

It is clear from Eq. (13) that the field amplitude in the middle waveguide is given by

$$e^{(\lambda_i - i\lambda_r)z}\alpha_1 b_1 + e^{(-\lambda_i - i\lambda_r)z}\alpha_2 b_2 + e^{-i\lambda_3 z}\alpha_3 b_3. \tag{14}$$

The second term in Eqs. (13) and (14) will decay rapidly. Therefore, for large propagation length, namely $z \gg \kappa$, the $\vec{\psi}(z)$ can be written approximately as

$$\vec{\psi}(z \gg \kappa) \approx e^{(\lambda_i - i\lambda_r)z}\alpha_1|\lambda_1\rangle + e^{-i\lambda_3 z}\alpha_3|\lambda_3\rangle \tag{15}$$

and the intensity in the middle waveguide is approximately given by

$$|A_2|^2 \approx |e^{(\lambda_i - i\lambda_r)z}\alpha_1 b_1 + e^{-i\lambda_3 z}\alpha_3 b_3|^2. \tag{16}$$

While in general there is not a closed form for the eigenvalues and eigenvectors of our system, one can calculate them numerically. Numerical analysis shows that if the system satisfies the AE condition in Eq. (8), then we have

$$b_{1,2}(\neq 0) \ll 1 \ll b_3. \tag{17}$$

In the exact phase where λ_i is zero, we conclude from Eq. (14) that the intensity of the middle waveguide remains almost constant and its value is given by $|A_2|^2 \approx |e^{-i\lambda_3 z}\alpha_3 b_3|^2 = |\alpha_3 b_3|^2$. However, in the broken phase, although $b_{1,2}(\neq 0) \ll 1$ for a large propagation length, we deduce from Eq. (16) that the intensity in the middle waveguide amplifies exponentially, namely $|A_2|^2 \approx |e^{(\lambda_i - i\lambda_r)z}\alpha_1 b_1|^2 = e^{2\lambda_i z}|\alpha_1 b_1|^2$. Therefore, in the broken phase the middle waveguide will not remain a dark state and its intensity keeps increasing exponentially.

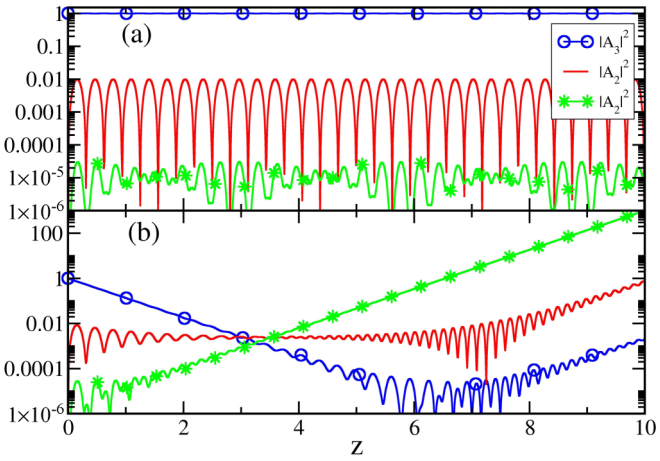

FIG. 5. (a) Beam dynamics in a Hermitian trimer shown in Fig. 1 with broken P-symmetry. The parameters are chosen such that field intensity remains mainly in waveguide A_3. (b) Similar to (a) with $\gamma = 1$. The system is in the broken phase, and the complex eigenvalues of the system cause an exponential growth in the field intensity of the middle waveguide.

While the above intuitive picture can be described mathematically, in the following we use a pedagogical and different approach to explain the nonconstant intensity dark state in the broken phase. Let us look for the condition in which the dark waveguide is either of the outer waveguides. In this case, from Eqs. (3) and (4), one finds that in addition to Eq. (6), another condition must be fulfilled:

$$|\kappa_{13}| \ll |\Delta\beta_{13}|. \tag{18}$$

If the system is Hermitian and P-symmetric, namely $\beta_1 = \beta_3$, then the above condition cannot be satisfied. However, if the system does not preserve the P operator, in other words $\beta_{13} \neq 0$, then one can choose the parameters of the system such that Eq. (18) is fulfilled. Figure 5 represents the field intensities at each waveguide when we excited the waveguide with propagation constant β_3. Here, we chose the normalized $\gamma = 1$; the relative propagation constants to be $\beta_1 = 20$, $\beta_2 = 40$, and $\beta_3 = 2$; and the couplings to be $\kappa_{13} = 0$. These chosen parameters satisfy both conditions in Eqs. (6) and (18), and thus we see that the field remains in the excited waveguide with fluctuations of the order of $\sim 10^{-2}$. We could make these fluctuations smaller by choosing larger values for β_2. However, this choice helps us to better understand the influence of gain and loss on the dynamics of the field. As depicted in Fig. 5, when we increase the gain and loss parameter γ in the system, although we do not violate the condition (18), the AE in terms of constant intensity in the dark state is no longer preserved, and the field intensity starts increasing in all waveguides. Note that because the real parts of the propagation constants in the outer waveguides are not the same, the structure enters into the broken phase with any small but nonzero γ. The complex component of the eigenvalues amplifies the fluctuations, and thus we observe that after $\approx$8 coupling units, the intensities in all waveguides start increasing exponentially. Consequently, one can conclude that AE is not preserved in the broken phase.

IV. CONCLUSION

We have shown that while AE is preserved in the exact phase, i.e., the intensity of the dark state remains constant, it does not hold in the broken phase where the intensity of the dark state increases exponentially. The existence of complex eigenvalues leads to an exponential growth of the intensity in all the waveguides, and thus the intensity of the dark state does not remain constant.

ACKNOWLEDGMENTS

H.R. gratefully acknowledge support from the UT system under the Valley STAR award.

[1] V. J. Sorger, Z. Ye, R. F. Oulton, Y. Wang, G. Bartal, X. Yin, and X. Zhang, Nat. Commun. **2**, 331 (2011).
[2] S. M. Spillane, T. J. Kippenberg, and K. J. Vahala, Nature (London) **415**, 621 (2002).
[3] E. Yablonovitch, J. Opt. Soc. Am. B **10**, 283 (1993).
[4] N. I. Zheludev and Y. S. Kivshar, Nat. Mater. **11**, 917 (2012).
[5] K. G. Makris, R. El-Ganainy, D. N. Christodoulides, and Z. H. Musslimani, Phys. Rev. Lett. **100**, 103904 (2008).
[6] C. E. Ruter, K. G. Makris, R. El-Ganainy, D. N. Christodoulides, M. Segev, and D. Kip, Nat. Phys. **6**, 192 (2010).
[7] L. Ge and H. E. Tureci, Phys. Rev. A **88**, 053810 (2013).
[8] P. Peng, W. Cao, C. Shen, W. Qu, J. W. Jiang, and Y. Xiao, Nat. Phys. **12**, 1139 (2016).
[9] J. Schindler, Z. Lin, J. M. Lee, H. Ramezani, F. M. Ellis, and T. Kottos, J. Phys. Math. Theor. **45**, 444029 (2012).
[10] X. Zhu, H. Ramezani, C. Shi, J. Zhu, and X. Zhang, Phys. Rev. X **4**, 031042 (2014).
[11] C. Shi, M. Dubois, Y. Chen, L. Cheng, H. Ramezani, Y. Wang, and X. Zhang Nat. Commun. **7**, 11110 (2016).
[12] H. Ramezani, M. Dubois, Y. Wang, Y. R. Shen, and X. Zhang, New J. Phys. **18**, 095001 (2016).
[13] R. Fleury, D. Sounas, and A. Alù, Nat. Commun. **6**, 5905 (2015).
[14] S. Longhi, J. Phys. A **44**, 485302 (2011).
[15] S. Longhi, Phys. Rev. Lett. **103**, 123601 (2009).
[16] A. Mostafazadeh, Phys. Rev. Lett. **110**, 260402 (2013).
[17] Y. D. Chong, L. Ge, and A. D. Stone, Phys. Rev. Lett. **106**, 093902 (2011).
[18] H. Schomerus, Opt. Lett. **38**, 1912 (2013).
[19] W. Chen, S. K. Ozdemir, G. Zhao, J. Wiersig, and L. Yang, Nature (London) **548**, 192 (2017).
[20] C. M. Bender and S. Boettcher, Phys. Rev. Lett. **80**, 5243 (1998).
[21] Z. Lin, H. Ramezani, T. Eichelkraut, T. Kottos, H. Cao, and D. N. Christodoulides, Phys. Rev. Lett. **106**, 213901 (2011).
[22] A. Regensburger, C. Bersch, M-A. Miri, G. Onishchukov, D. N. Christodoulides, and U. Peschel, Nature (London) **488**, 167 (2012).
[23] H. Schomerus and N. Y. Halpern, Phys. Rev. Lett. **110**, 013903 (2013).

[24] B. Peng, S. K. Ozdemir, S. Rotter, H. Yilmaz, M. Liertzer, F. Monifi, C. M. Bender, F. Nori, and L. Yang, Science **346**, 328 (2014).
[25] S. Malzard, C. Poli, and H. Schomerus, Phys. Rev. Lett. **115**, 200402 (2015).
[26] S. Weimann, M. Kremer, Y. Plotnik, Y. Lumer, S. Nolte, K. G. Makris, M. Segev, M. C. Rechtsman, and A. Szameit, Nat. Mater. **16**, 433 (2017).
[27] H. Ramezani, Phys. Rev. A **96**, 011802 (2017).
[28] A. V. Yulin and V. V. Konotop, Opt. Lett. **38**, 4880 (2013).
[29] M. Mrejen, H. Suchowski, T. Hatakeyama, C. Wu, L. Feng, K. O. Brien, Y. Wang, and X. Zhang, Nat. Commun. **6**, 7565 (2015).
[30] A. Guo, G. J. Salamo, D. Duchesne, R. Morandotti, M. Volatier-Ravat, V. Aimez, G. A. Siviloglou, and D. N. Christodoulides, Phys. Rev. Lett. **103**, 093902 (2009).
[31] H. Ramezani, J. Schindler, F. M. Ellis, U. Gunther, and T. Kottos, Phys. Rev. A **85**, 062122 (2012).